论著·基础医学

FABP4抑制剂BMS309403通过调控FABP4/PPAR-γ信号轴减轻肝肺综合征大鼠肝肺损伤

胡娅雯,陈 林,李伯龙,鲁开智,段家翔 陆军军医大学(第三军医大学)第一附属医院麻醉科,重庆

[摘要] **目的** 肝肺综合征(hepatopulmonary syndrome, HPS)以肺部炎症、肺血管扩张及新生为特征。肝硬化患者血清脂肪酸结合蛋白4(fatty acid binding protein 4, FABP4)水平升高与不良预后相关,且FABP4参与炎症与血管新生调控。通过建立胆总管结扎(bile duct ligation, BDL)诱导的HPS大鼠模型,采用FABP4抑制剂BMS309403进行干预,旨在探究FABP4/PPAR-γ信号轴在HPS发病中的作用,并评估抑制FABP4对肝肺损伤的保护机制。**方法** 将24只6~8周龄的SPF级雄性SD大鼠(体质量200~220 g),按随机数字表法分为(n=6):假手术对照组(Sham组)、BDL术后3周组(BDL3W组)、BDL术后5周组(BDL5W组)和BDL+BMS309403治疗组(BDLB组)。BDL3W、BDL5W及BDLB组通过BDL建立HPS模型,Sham组仅进行胆总管游离。BDLB组自术后第15天起,每周2次腹腔注射BMS309403(5 mg/kg),持续3周。BDL3W组在术后第3周取材,Sham、BDL5W及BDLB组则在术后第5周取材。通过HE染色评估肝肺组织的病理变化,Masson三色染色评估肝脏纤维化程度,油红O染色用于检测肝脏脂质堆积。对Sham组和BDL3W组的肺组织进行基因芯片检测,对差异表达基因进行整合分析,包括:基于特定基因集的表达谱热图绘制、差异表达火山图可视化以及GO功能富集分析。通过免疫组化检测肺组织中CD31、iNOS、TNF-α、NF-κB p65及PPAR-γ的表达情况。免疫荧光用于检测肺组织中FABP4的定位及其表达水平。Western blotting用于定量检测肺组织中FABP4和PPAR-γ的蛋白水平。动脉血气分析用于检测PaO_2和P(A-a)O_2水平以评估肺功能,血清生化检测ALT和AST以评估肝功能。**结果** ①与BDL3W组相比,BDL5W组大鼠肝脏结构进行性紊乱,纤维化逐渐加重,相对胶原面积显著增加(P<0.01);血清ALT水平自Sham组至BDL3W组、BDL5W组持续升高(P<0.01),AST呈同样趋势(P<0.01)。肺组织炎性细胞浸润进行性加重,PaO_2自Sham组至BDL3W组、BDL5W组逐渐下降(P<0.05);与BDL3W组相比,P(A-a)O_2在BDL5W组明显升高(P<0.01),证实HPS模型建立成功。②BDL3W组肺组织FABP4基因显著上调(FC≥1.5,P≤0.05),GO富集分析显示脂代谢相关基因显著富集,提示FABP4和脂代谢在HPS肺部病变中发挥重要作用。③与BDL5W组相比,BDLB组血清AST和ALT水平均显著降低(P<0.01),同时肝纤维化改善,表现为相对胶原面积显著减小(P<0.01)。肺部炎性浸润、出血及肺不张减轻,PaO_2显著升高(P<0.01),P(A-a)O_2显著下降(P<0.01)。④免疫荧光及Western blotting显示BDLB组肺组织FABP4表达较BDL5W组降低(P<0.05),免疫组化及Western blotting显示BDLB组肺组织PPAR-γ表达较BDL5W组显著升高(P<0.05)。⑤与BDL5W组相比,BDLB组肝脏脂滴堆积减少,免疫组化显示肺微血管管腔直径显著减小(P<0.01),iNOS表达显著下调(P<0.01),炎症因子TNF-α和NF-κB p65表达均显著降低(P<0.01)。**结论** FABP4抑制剂BMS309403可通过调控FABP4/PPAR-γ信号轴,改善肝脏脂代谢紊乱,抑制NF-κB p65/TNF-α介导的肺部炎症反应和iNOS/NO驱动的肺微血管扩张,从而减轻HPS大鼠的肝肺病理损伤并改善低氧血症。

[关键词] 肝肺综合征;脂肪酸结合蛋白4;过氧化物酶体增殖激活受体-γ
[中图法分类号] R563;R575;R963 [文献标志码] A

[基金项目] 国家自然科学基金面上项目(82270656);重庆市自然科学基金面上项目(CSTB2023NSCQ-MSX0598)

[通信作者] 鲁开智,E-mail: lukaizhi2010@163.com
段家翔,E-mail: duanjiaxiang@tmmu.edu.cn

2097-0927/Copyright © 2026, 陆军军医大学(第三军医大学)。这篇开放获取文章遵循CC BY许可协议(https://creativecommons.org/licenses/by/4.0/)

引用格式:胡娅雯,陈林,李伯龙,等. FABP4抑制剂BMS309403通过调控FABP4/PPAR-γ信号轴减轻肝肺综合征大鼠肝肺损伤[J]. 陆军军医大学学报,2026,48(09):1228-1240. DOI:10.16016/j.2097-0927.202601126.

Citation: HU Y W, CHEN L, LI B L, *et al*. FABP4 inhibitor BMS309403 attenuates hepatopulmonary injury in rats with hepatopulmonary syndrome through regulating the FABP4/PPAR-γ axis[J]. J Army Med Univ, 2026, 48(09): 1228-1240. DOI: 10.16016/j.2097-0927.202601126.

FABP4 inhibitor BMS309403 attenuates hepatopulmonary injury in rats with hepatopulmonary syndrome through regulating the FABP4/PPAR-γ axis

HU Yawen, CHEN Lin, LI Bolong, LU Kaizhi, DUAN Jiaxiang Department of Anesthesiology, First Affiliated Hospital, Army Medical University (Third Military Medical University), Chongqing, China

[**Abstract**] Objective Hepatopulmonary syndrome (HPS) is characterized by inflammation, pulmonary vasodiation and angiogenesis. Elevated serum level of fatty acid binding protein 4 (FABP4) in patients with liver cirrhosis is associated with poor prognosis, and FABP4 is involved in the regulation of inflammation and angiogenesis. Using a bile duct ligation (BDL)-induced HPS rat model and the FABP4 inhibitor BMS309403 for intervention, this study aims to investigate the role of the FABP4/PPAR-γ signaling axis in the pathogenesis of HPS and to evaluate the protective mechanism of FABP4 inhibition against hepatopulmonary injury. Methods A total of 24 male SPF SD rats (6 to 8 weeks old, weighing 200 to 220 g) were enrolled and randomly divided into (n=6): a sham operation group (Sham group), the BDL postoperative 3-week group (BDL3W group), the BDL postoperative 5-week group (BDL5W group), and a BDL+BMS309403 treatment group (BDLB group). The BDL3W, BDL5W and BDLB groups underwent BDL to establish an HPS model, while the Sham group underwent only bile duct manipulation without ligation. The BDLB group received intraperitoneal injections of BMS309403 (5 mg/kg, twice per week) from postoperative day 15 for 3 weeks. The BDL3W group was sacrificed at week 3 post-surgery, while the Sham, BDL5W, and BDLB groups were sacrificed at week 5 post-surgery. Histopathological changes in the liver and lung tissues were evaluated using HE staining. The severity of hepatic fibrosis was assessed by Masson's trichrome staining, while hepatic lipid accumulation was examined using Oil Red O staining. Microarray was performed on lung tissues from the Sham and BDL3W groups, and integrated analysis of differentially expressed genes (DEGs) was conducted, including: heatmap plotting based on specific gene sets, visualization of differential expression with volcano plots, and GO functional enrichment analysis. Immunohistochemistry was used to detect the localization and expression levels of CD31, iNOS, TNF-α, NF-κB p65, and PPAR-γ in lung tissues. Immunofluorescence staining was performed to determine the expression of FABP4. The protein levels of FABP4 and PPAR-γ in lung tissues were quantified by Western blotting. Arterial blood gas analysis was conducted to measure PaO_2 and $P(A\text{-}a)O_2$ for the evaluation of pulmonary function, and serum levels of ALT and AST were determined to evaluate hepatic function. Results ① Compared with the BDL3W group, the BDL5W group exhibited progressively disorganized liver structure, gradually aggravated fibrosis, and a significant increase in relative collagen areas (P<0.01). Serum ALT levels increased continuously from the Sham group to the BDL3W and BDL5W groups (P<0.01), with AST levels showing the same trend (P<0.01). In the lungs, inflammatory cell infiltration aggravated progressively, and PaO_2 decreased gradually from the Sham to BDL3W and BDL5W groups (P<0.05). Compared with the BDL3W group, $P(A\text{-}a)O_2$ was markedly elevated in the BDL5W group (P<0.01), confirming the successful establishment of the HPS model. ② In the BDL3W group, FABP4 gene was significantly upregulated in the lung tissues (FC≥1.5, P≤0.05). GO enrichment analysis revealed significant enrichment of lipid metabolism-related genes, suggesting that FABP4 and lipid metabolic processes play important roles in the pulmonary pathogenesis during HPS. ③Compared with the BDL5W group, the BDLB group showed significantly decreased serum AST and ALT levels (P<0.01), accompanied by attenuated hepatic fibrosis, as evidenced by a significant reduction in relative collagen area (P<0.01). Pulmonary inflammatory infiltration, hemorrhage, and atelectasis were alleviated, with a significant increase in PaO_2 (P<0.01) and an obvious decrease in $P(A\text{-}a)O_2$ (P<0.01). ④ Immunofluorescence and Western blotting revealed that FABP4 expression in the lung tissues of the BDLB group was significantly lower than that in the BDL5W group (P<0.05). Immunohistochemistry and Western blotting further demonstrated

that PPAR-γ expression in the lung tissues was significantly enhanced in the BDLB group compared with the BDL5W group (P<0.05). ⑤ Compared with the BDL5W group, the BDLB group exhibited reduced hepatic lipid droplet accumulation. Immunohistochemical analysis showed a significant decrease in the diameter of pulmonary microvascular lumens (P<0.01), along with significantly downregulated expression of iNOS (P<0.01), and remarkably reduced expression levels of the inflammatory factors TNF-α and NF-κB p65 (P<0.01). **Conclusion** The FABP4 inhibitor BMS309403 ameliorates hepatopulmonary pathological injury and improves hypoxemia in HPS rats by modulating the FABP4/PPAR-γ signaling axis, ameliorating hepatic lipid metabolism disorder, inhibiting NF-κB p65/TNF-α-mediated pulmonary inflammatory response, and suppressing iNOS/NO-driven pulmonary microvascular dilation.

[**Key words**] hepatopulmonary syndrome; fatty acid-binding protein 4; peroxisome proliferator-activated receptor gamma

Supported by the General Program of National Natural Science Foundation of China (82270656) and the General Project of Natural Science Foundation of Chongqing (CSTB2023NSCQ-MSX0598). Corresponding authors: LU Kaizhi, E-mail: lukaizhi2010@163.com; DUAN Jiaxiang, E-mail: duanjiaxiang@tmmu.edu.cn

肝肺综合征(hepatopulmonary syndrome, HPS)是一种严重的以慢性肝病及门脉高压为基础的肺血管并发症,以肺血管扩张(intrapulmonary vascular dilatations, IPVD)和血管新生导致氧合障碍为特征,临床表现为直立性低氧血症和呼吸困难,发病率占肝硬化患者的15%~30%[1-2]。HPS呈进行性发展,1年病死率高达41%[3]。HPS发病机制涉及4个核心环节:肺血管舒缩障碍、细菌易位与肺部炎症、血管新生与分流形成、肺泡功能障碍[4]。目前公认的治疗HPS的唯一有效手段是肝移植,然而晚期合并严重肺功能障碍的HPS患者肝移植手术的失败率和围术期并发症均显著增高[5]。因此,早期识别和干预慢性肝病患者肺部病理改变,是保障HPS患者顺利度过肝移植围术期、改善预后的关键。

脂肪酸结合蛋白4(fatty acid binding protein 4, FABP4)是脂肪酸结合蛋白家族的一员,主要由脂肪细胞、巨噬细胞产生,作为脂质伴侣介导游离脂肪酸等物质转运到不同细胞器发挥相应作用[6]。FABP4涉及的生物学过程包括脂肪酸运输、脂解调节、胆固醇代谢[7]、炎症信号[8-10]和血管新生[11-12],在多种疾病的病理生理变化中发挥重要作用。研究发现肝硬化患者血清FABP4显著升高,其升高水平与肝硬化并发症、急性慢性肝衰竭及生存率低相关[13]。BMS309403是一种选择性的FABP4抑制剂,它通过可逆地与FABP4脂肪酸结合口袋结合,抑制FABP4与内源性配体(如长链脂肪酸和氧化脂质)结合的能力[14],在调节脂质代谢、炎症反应和细胞存活等多个生物学过程中发挥作用,并且在多种疾病(如代谢紊乱、器官纤维化和癌症等)中展现出治疗潜力[15-17]。然而BMS309403能否通过抑制FABP4改善HPS的相关病理表现目前尚不清楚。因此,本研究拟建立胆总管结扎(bile duct ligation, BDL)诱导的HPS大鼠模型,评价FABP4抑制剂BMS309403对肝肺病理损伤、炎症因子及脂质代谢的影响,探讨相关调控机制,为HPS临床治疗提供新的思路。

1 材料与方法

1.1 实验材料

1.1.1 实验动物伦理与分组 本实验获得第三军医大学实验动物福利伦理审查委员会批准(AMUWEC20224009)。所有动物在SPF级屏障系统中饲养,环境参数如下:温度控制在(23±1)℃,相对湿度为50%±5%,光照周期为12 h/12 h,自由摄食、饮水。为减少动物痛苦,所有手术及术后处理采用无菌技术,并在麻醉下进行。实验期间每日监测动物活动状态及切口愈合情况,每3日监测动物的体质量,未发生预期外的严重不良事件。出现以下任一情况即对动物实施安乐死:①体质量下降超过基础体质量的20%;②出现严重呼吸困难、无法自主进食饮水;③出现无法缓解的剧烈疼痛表现(如持续蜷缩、尖叫等)。本研究选用24只6~8周龄SPF级雄性SD大鼠(初始体质量200~220 g),购自陆军军医大学实验动物中心。采用随机数字表法将大鼠分为4组(n=6):假手术对照组(Sham组)、BDL术后3周组(BDL3W组)、BDL术后5周组(BDL5W组)和BDL+BMS309403治疗组(BDLB组)。

1.1.2 主要试剂 BMS309403购自美国MCE公司;大鼠单抗PPAR-γ购自中国SciBen公司;兔抗FABP4购自中国ABclonal公司;兔抗iNOS、兔抗核因子-κB p65

(NF-κB p65)、鼠抗CD31购自美国abcam公司;鼠抗TNF-α购自中国Bioss公司;BCA蛋白定量分析试剂盒、Supersignal™-WestFemto超敏底物购自美国Thermo Fisher公司;PVDF膜购自德国Merk公司。

1.2 实验方法

1.2.1 HPS动物模型建立与BMS309403干预处理 大鼠禁食8 h后,采用小型动物麻醉机(RWD,中国)以2%异氟烷持续吸入诱导麻醉。待麻醉生效后,BDL3W、BDL5W和BDLB组行改良胆总管结扎术,Sham组仅游离胆总管后逐层关腹。术毕将大鼠置于恒温保温箱中待其自然苏醒,随后按实验计划常规饲养。BDLB组自术后第15天起给予BMS309403腹腔注射干预(5 mg/kg,每周2次),连续3周。

1.2.2 大鼠肝肺组织及血液样本采集 各组取材时间安排如下:BDL3W组于术后第3周末取材;Sham、BDL5W、BDLB组于术后第5周末取材。取材当日动物腹腔注射2%戊巴比妥钠(0.2 mL/100 g)进行麻醉。麻醉充分后,经腹主动脉采集动脉血约8 mL,其中0.5 mL动脉血血样用于血气分析;采血结束后,于右心耳剪开一小口作为引流口,经右心室以肝素化生理盐水持续灌注肺循环系统,直至右心耳流出液澄清且肝脏由暗红色逐渐变白(提示灌注充分)。随后完整取下肝脏及肺组织并拍照留存。继而分离肝脏最大叶及右肺组织,立即液氮速冻后转移至-80 ℃冰箱保存,用于后续分子生物学实验;另取部分肝组织及左肺组织置于4%多聚甲醛溶液中固定≥24 h,用于组织病理学分析。

1.2.3 血气分析仪检测大鼠动脉血PaO_2、P(A-a)O_2水平 腹主动脉穿刺采集的动脉血0.5 mL,注入预肝素化注射器中,排除气泡密封后于10 min内送检。使用Radiometer ABL90 FLEX血气分析仪检测PaO_2、P(A-a)O_2。

1.2.4 全自动生化分析仪检测大鼠血清ALT和AST水平 大鼠腹主动脉血液置于肝素抗凝管中,室温静置2 h后,在4 ℃下以4 000 r/min离心20 min。收集上清液后,采用Mindray BS-240vet全自动生化分析仪检测血清ALT和AST水平。

1.2.5 HE染色检测大鼠肝肺组织学改变 肝肺组织经多聚甲醛固定24 h后常规石蜡包埋,切片二甲苯脱蜡,梯度乙醇复水;苏木精染核5 min,盐酸酒精分化5~10 s并蓝化,伊红染色2 min。脱水、透明后用中性树胶封片,光学显微镜观察并拍照。

1.2.6 Masson三色染色检测大鼠肝组织纤维化 肝组织石蜡切片常规脱蜡水化。Weigert铁苏木精染核10 min,1%盐酸酒精分化至背景清晰,流水蓝化。Biebrich Scarlet染胞浆5 min,磷钨酸处理5 min。苯胺蓝染胶原5 min,1%醋酸冲洗。梯度乙醇脱水,二甲苯透明,中性树胶封片。镜下结果判读:胶原纤维呈蓝色,肌纤维及胞浆呈红色。

1.2.7 油红O染色检测评估肝脏脂代谢 新鲜肝组织OCT包埋,-20 ℃速冻10 min,冰冻切片,室温晾干15 min。丙酮固定5 min,0.5%油红O染液(60%异丙醇配制)避光染色10 min(镜下脂滴鲜红即止),60%异丙醇分化至背景透明,蒸馏水洗。1%苏木精复染核2 min,流水蓝化5 min,0.1%盐酸酒精分化5~10 s,水洗后甘油封片。

1.2.8 免疫组化定量分析肺组织iNOS、TNF-α、NF-κB p65、PPAR-γ与血管相关蛋白CD31 大鼠肺组织石蜡切片常规脱蜡水化后行抗原修复,3%H_2O_2孵育30 min淬灭内源性过氧化物酶,10%山羊血清封闭1 h。一抗4 ℃孵育过夜:兔抗iNOS(1∶200)、鼠抗CD31(1∶200)、鼠抗TNF-α(1∶200)、兔抗NF-κB p65(1∶200)、鼠抗PPAR-γ(1∶300)。PBS洗涤后,二抗室温孵育1 h,DAB显色,苏木精复染核,中性树胶封片。由1名对实验分组不知情的评估员,在每张切片中随机选取5个具有代表性的区域,采用Image J软件分析阳性细胞面积并进行统计分析。

1.2.9 免疫荧光定量分析肺组织FABP4蛋白 石蜡切片常规脱蜡水化后行抗原修复,3%BSA封闭。兔抗FABP4一抗4 ℃孵育过夜,PBS洗涤后加HRP标记二抗室温孵育,DAPI复染核,抗荧光猝灭封片剂封片。荧光显微镜观察并采集图像。

1.2.10 Western blotting检测肺组织FABP4及PPAR-γ蛋白 取大鼠肺组织加预冷RIPA裂解液超声破碎,冰上裂解离心获取总蛋白,BCA法定量后调整浓度至4 μg/μL。每孔上样40 μg/10 μL,根据目标蛋白分子量选择凝胶浓度:15 kDa用12.5%、52 kDa用10%。PVDF膜预活化后,在甘氨酸转膜液中恒流转膜。5%脱脂奶粉TBST封闭,一抗4 ℃过夜。HRP二抗(1∶5 000)室温孵育,TBST洗涤后ECL显影成像。

1.2.11 特定基因表达谱的热图分析 从基因表达谱数据中提取特定基因的表达值进行可视化分析。使用R语言,筛选出25个目标基因,对每个基因在各样本中的表达值进行标准化(Z-score转换),消除基因间表达量级差异。使用Complex Heatmap包绘制热图,颜色梯度设置为蓝色(低表达)到白色(中等表达)

再到红色(高表达),对基因进行层次聚类。

1.2.12 差异表达基因的火山图可视化 分析使用Sham组与BDL3W组比较的差异表达数据,通过火山图展示基因表达变化,计算Log_2FC和$-Log_{10}P$。设定显著性阈值:FC≥1.5且P≤0.05。使用ggplot2包绘制火山图,显著上调基因标记为红色,显著下调基因标记为蓝色,不显著基因显示为灰色。特别标记FABP4基因。

1.2.13 差异表达基因的GO功能富集分析 采用Metascape与微生信平台对差异表达基因进行GO功能富集分析。筛选差异基因($|Log_2FC|$>0.8且FDR<0.05),并去除重复。将差异基因上传至Metascape网站(https://metascape.org)进行富集分析,采用超几何检验并对多重比较进行Benjamini-Hochberg校正,以P<0.05为显著标准,并输出富集条目及网络图。同期在微生信平台(https://www.bioinformatics.com.cn)导入同一基因集,选择GO富集模块,获得气泡图等可视化结果。

1.3 统计学分析

所有实验独立重复3次。采用GraphPad Prism 9.0软件进行统计分析。计量资料以$\bar{x}\pm s$表示,多组间比较采用单因素方差分析,检验水准为:α=0.05。

2 结果

2.1 BDL导致大鼠肝肺组织病理损伤进行性加重并伴恶化动脉血气及血清肝酶指标

与Sham组相比,BDL3W及BDL5W组肝肺组织大体图片显示:肺表面由散在出血点发展为弥漫黄褐色斑点;同时,肝脏由颜色加深、表面略粗糙进展至肝脏体积缩小、质地僵硬、表面呈黄色伴弥漫性小结节(图1A)。肺HE染色显示:与Sham组相比,BDL3W组肺组织可见少量炎性细胞浸润,部分肺泡腔不张;BDL5W组肺组织大量炎性细胞浸润,肺泡结构破坏,肺泡腔及肺间质散在出血点,提示肺损伤随胆管结扎时间显著进展(图1B)。肝HE染色显示:肝小叶结构由相对完整、肝细胞相对排列规则(BDL3W组)逐渐演变为结构紊乱伴小胆管大量增生扩张(BDL5W组),提示肝细胞损伤加重(图1C)。肝Masson染色及相对胶原面积定量分析表明:与BDL3W组相比,BDL5W组大鼠肝脏结构进行性紊乱,纤维化逐渐加重,相对胶原面积显著增加(P<0.01,图1D、E)。血气分析显示:PaO_2自Sham组至BDL3W组、BDL5W组逐渐下降(P<0.05),而与BDL3W组相比,$P(A\text{-}a)O_2$在BDL5W组明显升高(P<0.01),提示肺氧合功能显著受损(图1F、G)。肝功能指标显示:AST及ALT水平自Sham至BDL3W、BDL5W持续升高(P<0.01),进一步证实胆管结扎诱导的进行性肝功能损伤(图1H、I)。综合上述结果,BDL可导致进行性加重的肝纤维化和肝功能障碍,并伴随明显的结构性和功能性肝肺损伤。

2.2 BDL3W大鼠肺组织基因芯片鉴定出脂代谢关键基因FABP4显著上调

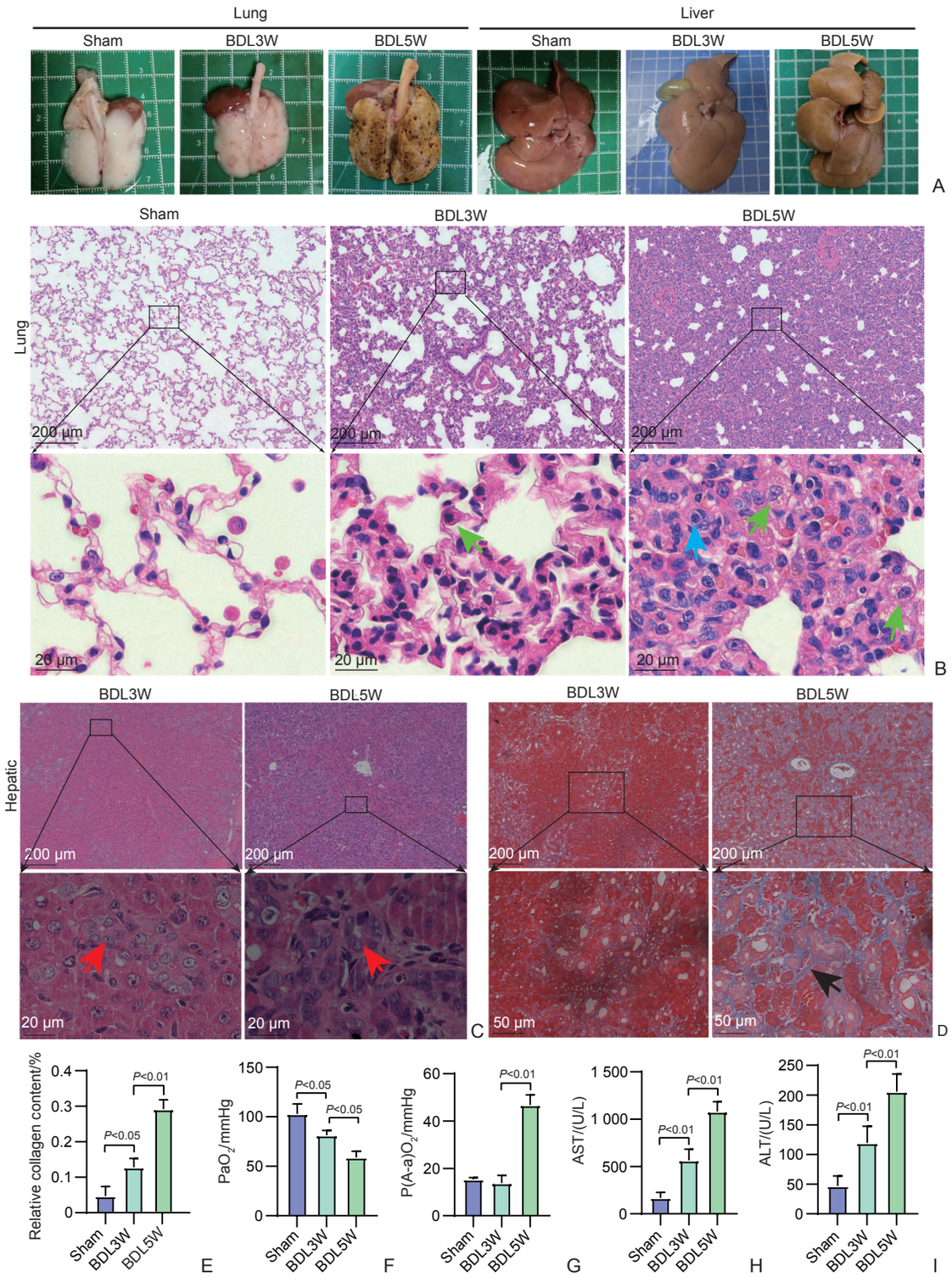
对Sham、BDL3W组大鼠肺组织进行基因芯片检测,经严格筛选(FC≥1.5且P≤0.05),FABP4在BDL3W组中被鉴定为显著上调基因之一(图2A、B)。同时,GO富集分析显示关键的富集生物过程包括免疫和炎症反应、血管生成以及脂质代谢(图2C),而FABP4正好是脂代谢通路中的关键调控因子。此外,肝硬化患者血清FABP4水平与肝硬化并发症严重程度及患者预后显著相关,并且FABP4在HPS病理机制核心环节(肺部炎症反应及肺血管新生)中发挥重要作用。基于上述证据,推测FABP4可能是连接慢性肝病与HPS肺部病变的潜在枢纽,因此拟选择FABP4作为干预靶点进行进一步的实验验证。

2.3 BMS309403干预显著减轻BDL大鼠肺组织与肝组织病理损伤并改善动脉血气及血清肝酶指标

HE染色显示,与BDL5W组相比,BDLB组大鼠肺部炎性细胞浸润程度、肺出血、肺不张、肺实变程度均减轻(图3A),肝组织结构紊乱、纤维化、胆管扩张程度等病理改变得到明显改善(图3B~D)。血气分析及血清生化结果显示,与BDL5W组相比,BDLB组动脉血PaO_2水平显著升高(P<0.01),$P(A\text{-}a)O_2$显著下降(P<0.01),血清ALT水平显著降低(P<0.01),AST亦明显降低(P<0.01,图3E~H)。综上,BMS309403干预可改善BDL诱导的肝肺损伤。

2.4 FABP4抑制剂BMS309403有效下调BDL大鼠肺组织FABP4蛋白表达并上调PPAR-γ表达

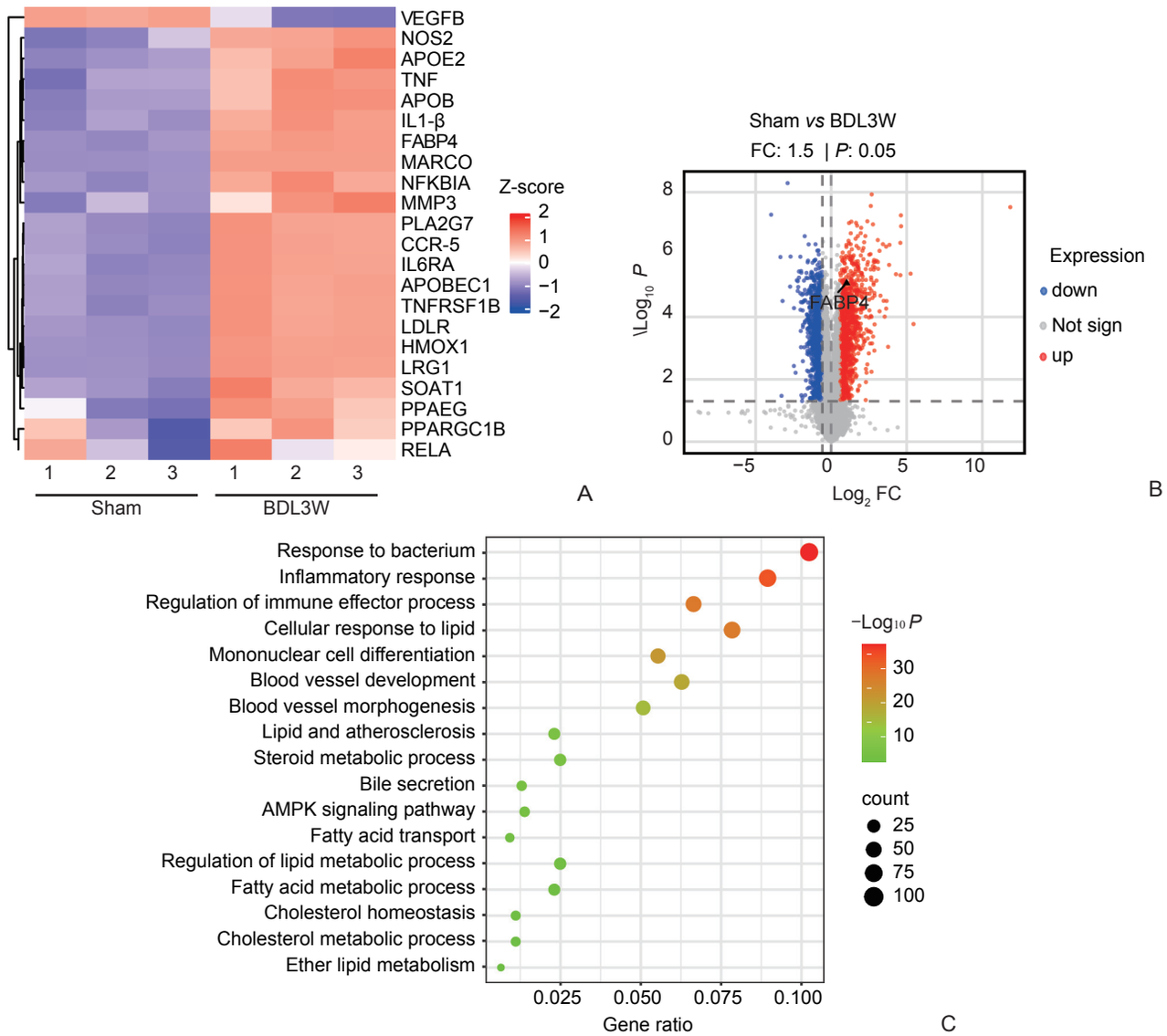
为了验证基因芯片分析结果,采用FABP4抑制剂BMS309403经腹腔注射对BDL大鼠进行处理。肺组织免疫荧光染色显示BDLB组FABP4的平均荧光强度较CBDL5W组降低(P<0.01,图4A、B);与BDL5W组相比,BDLB组PPAR-γ阳性细胞比例显著增加(P<0.01,图4C、D)。另外Western blotting检测结果也表明,与BDL5W组相比,BDLB组FABP4表达水平显著降低(P<0.05),PPAR-γ的总体表达水平升高(P<0.05,图4E~G)。上述结果提示,BMS309403干预可有效降低HPS大鼠肺组织中FABP4的表达水平,同时抑制FABP4可上调PPAR-γ表达,减轻HPS大鼠的肝肺损伤。



A: Representative gross morphological images of lung and liver specimens from Sham, BDL3W, and BDL5W rats; B and C: Representative photomicrographs of HE-stained sections demonstrating histopathological alterations in lung and hepatic parenchyma. Blue arrows: infiltrated lymphocytes, green arrows: infiltrated macrophages, red ones proliferative bile ductules; D: Representative Masson's trichrome-stained liver sections for assessment of fibrosis severity. Black arrows: collagen fiber deposition (blue-stained areas); E: Quantitative assessment of hepatic collagen content; F and G: Statistical analysis of arterial partial pressure of oxygen and alveolar-arterial oxygen partial pressure difference in the Sham, BDL3W and BDL5W rats; H and I: Statistical analysis of serum AST and ALT levels in the Sham, BDL3W and BDL5W rats

图1 BDL不同时间对肺肝组织病理、血气及肝功能指标的影响

Figure 1 Influence of different BDL durations on lung and liver morphologies, blood gas parameters and liver function indicators



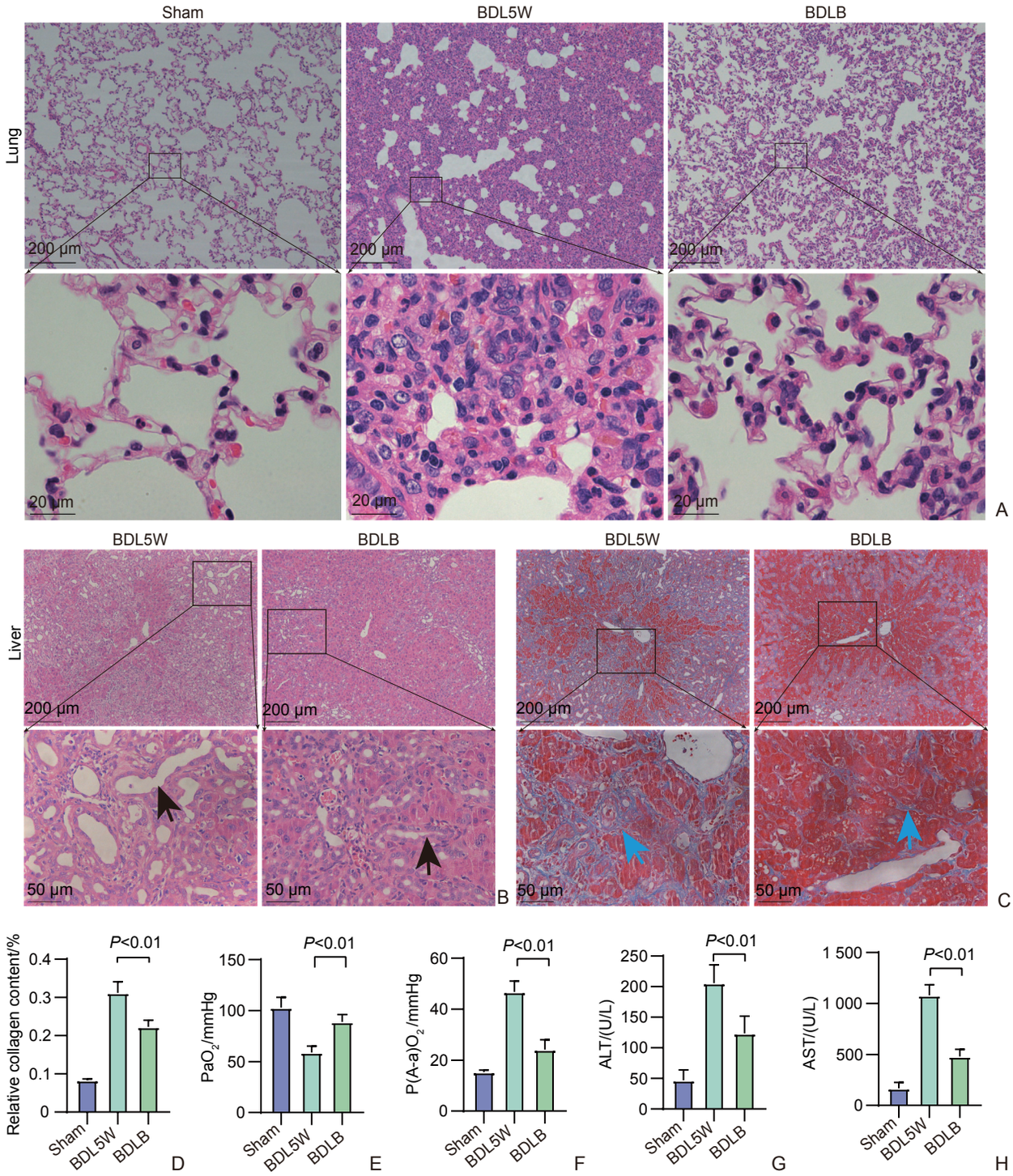
A: Heatmap illustrating the expression profiles of 25 target genes in lung tissue (Z-score normalized, hierarchical clustering); B: Volcano plot showing differentially expressed genes between BDL3W and Sham groups; C: GO enrichment analysis

图2 BDL大鼠肺组织基因芯片检测结果及GO分析

Figure 2 Microarray results and GO analysis of lung tissues in BDL rats

2.5 BMS309403通过改善肝脏脂质堆积、缓解肺微血管扩张并抑制NF-κB/TNF-α炎症通路,从而减轻BDL大鼠的肝肺损伤

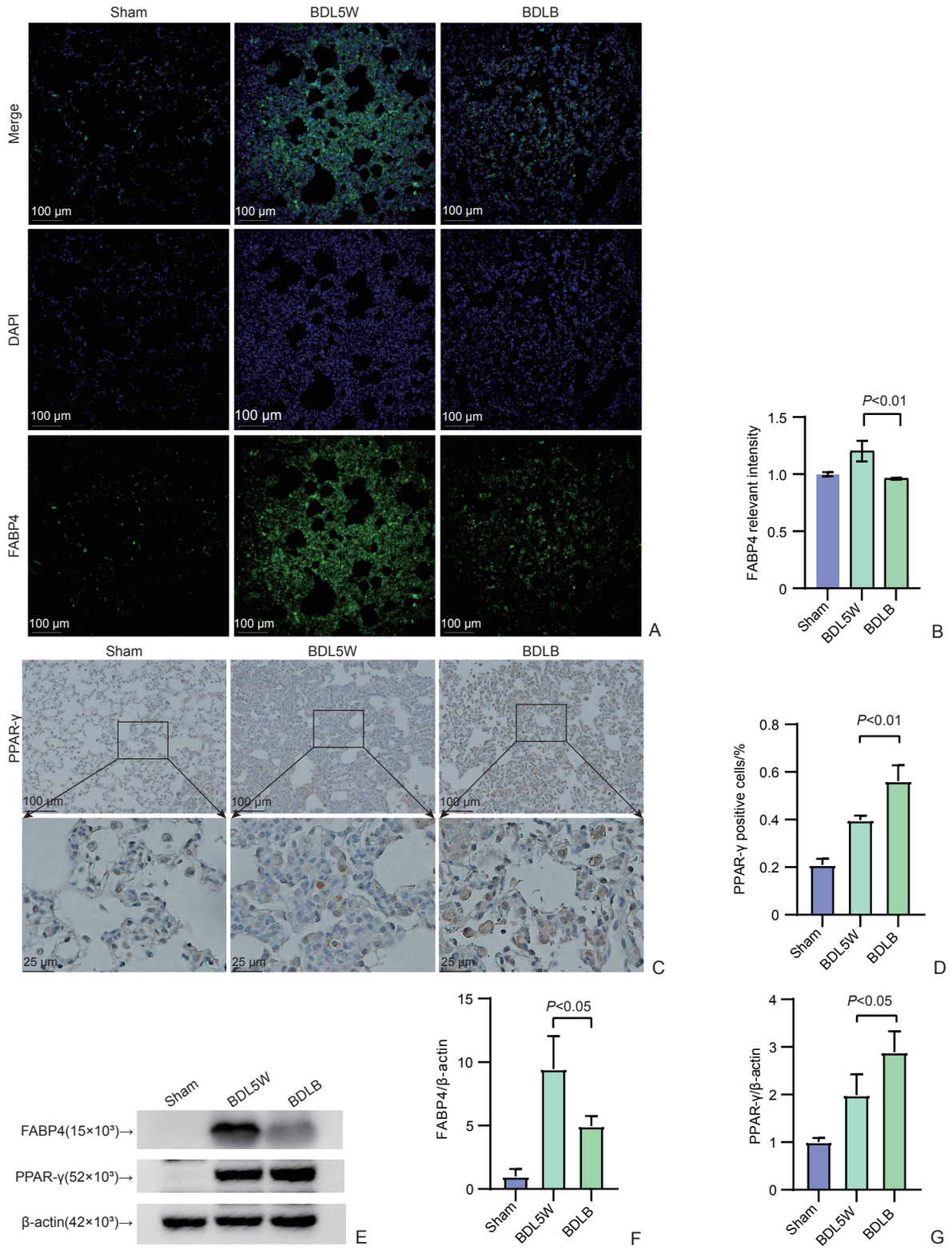
肝脏油红O染色显示:Sham组肝脏组织染色较浅,仅在肝细胞周围可见少量小的脂滴(红色染色区域)。相比之下,BDL5W组肝脏组织呈现明显的深红色染色,脂滴数量显著增多且体积增大,广泛分布于肝细胞内尤其是在中央静脉周围区域。而BDLB组脂滴数量和体积明显减小,提示BMS309403减轻了BDL大鼠肝脏的脂质堆积,改善了脂代谢紊乱(图5A)。肺组织CD31染色显示BDL5W组微血管管腔直径增大,血管扩张;给予BMS309403后,肺微血管管腔直径明显减小($P<0.01$),血管扩张得到缓解(图5B、C)。进一步通过肺组织iNOS免疫组化染色显示,与BDL5W组相比,BDLB组iNOS表达水平显著降低($P<0.01$,图5D、E),表面肺微血管扩张改善与NO等扩血管因子生成减少有关。此外,与BDL5W组相比,BDLB组肺组织TNF-α及NF-κB p65表达水平在BMS309403干预后显著降低($P<0.01$,图5F~I),提示BMS309403通过抑制NF-κB p65/TNF-α通路减轻了BDL大鼠炎症反应。



A and B: Representative HE staining images showing parenchymal pathological changes in rat lung and liver tissues. Black arrows: dilated bile ductules; C: Masson staining assessment of hepatic fibrosis in different groups. Blue arrow: collagen fiber deposition (blue staining); D: Statistical comparison of relative collagen content in liver tissues among 3 groups; E and F: Statistical comparison of PaO_2 and $P(A\text{-}a)O_2$ among groups; G and H: Statistical comparison of ALT and AST levels among groups

图3 BMS309403干预对肺肝组织病理、血气及肝功能指标的影响

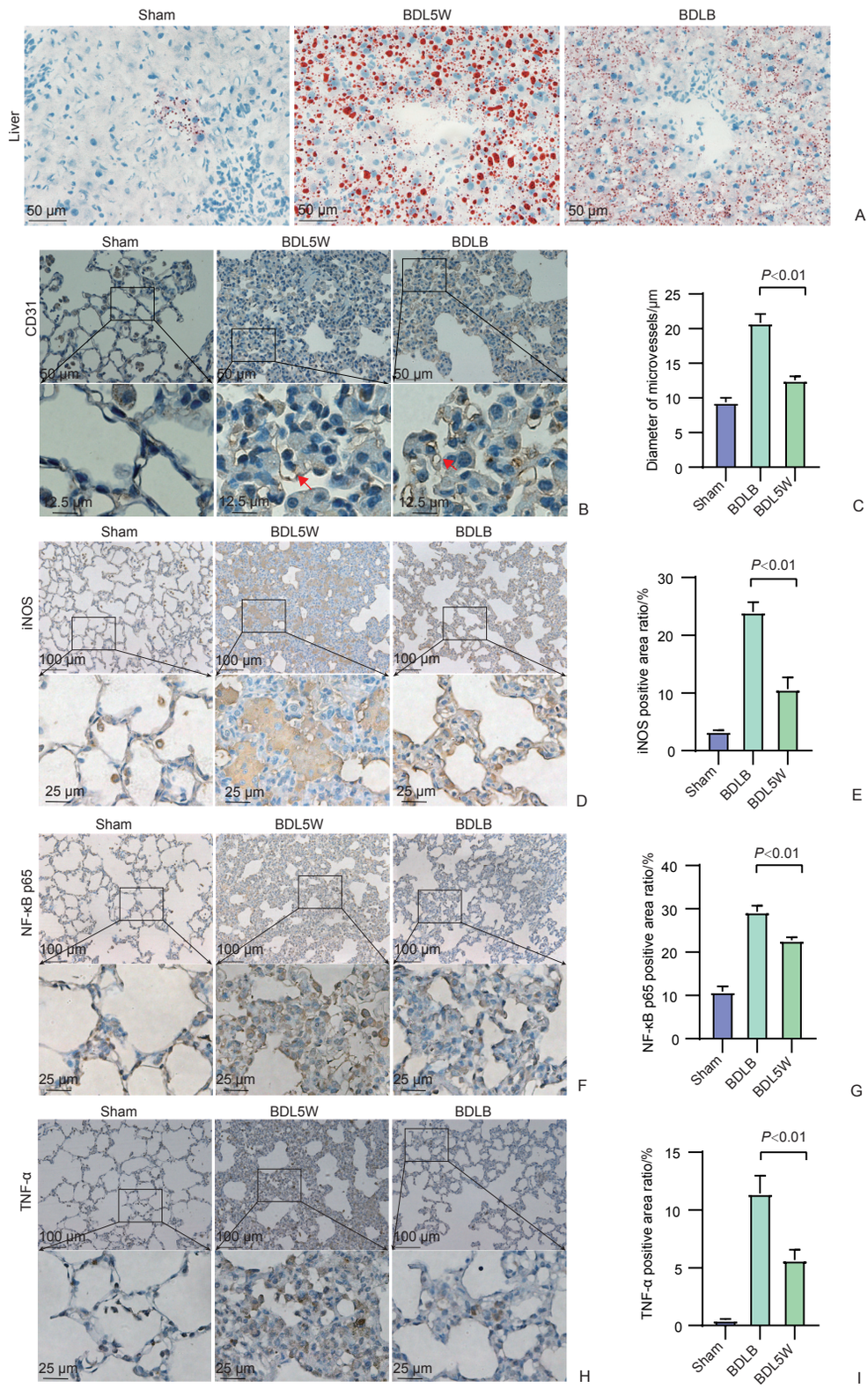
Figure 3 Influence of BMS309403 intervention on pathological features of lung and liver tissues, blood gas parameters and liver function indicators



A: Representative immunofluorescence staining images of FABP4 in lung tissues from the Sham, BDL5W and BDLB rats; B: Statistical analysis of FABP4 relevant fluorescence intensity in lung tissues; C: Representative immunohistochemical staining images of PPAR-γ in lung tissues from the Sham, BDL5W and BDLB rats; D: Statistical analysis of the percentage of PPAR-γ positive cells in lung tissues; E: Western blotting analysis of FABP4 and PPAR-γ protein expression in lung tissues; F and G: Statistical analysis of relative FABP4/β-actin protein and PPAR-γ/β-actin protein expression in lung tissues

图4 BMS309403干预对BDL大鼠肺组织中FABP4与PPAR-γ表达的影响

Figure 4 Effects of BMS309403 intervention on the expression of FABP4 and PPAR-γ in lung tissues of BDL rats



A: Lipid droplet accumulation in liver tissues as revealed by Oil Red O staining; B and C: Immunohistochemical staining and diameter analysis of CD31-positive microvessels in lung tissues; D and E: Immunohistochemical staining and quantification of iNOS-positive areas in lung tissues; F and G: Immunohistochemical staining and quantification of NF-κB p65-positive areas in lung tissues; H and I: Immunohistochemical staining and quantification of TNF-α-positive areas in lung tissues

图5 BMS309403对BDL大鼠肝脂代谢、肺微血管重塑及炎症反应的影响

Figure 5 Effects of BMS309403 on hepatic lipid metabolism, pulmonary microvascular remodeling, and inflammatory responses in BDL rats

3 讨论

本研究通过BDL成功建立HPS大鼠模型,并证实FABP4抑制剂BMS309403可显著减轻HPS大鼠的肝肺组织病理损伤,缓解低氧血症、改善肝功。现就上述发现,从脂代谢紊乱、FABP4/PPAR-γ信号轴调控、炎症与肺血管病变等3个层面展开讨论。

3.1 抑制FABP4通过减轻BDL大鼠肝脏脂质堆积与脂毒性,从而改善肝功能并削弱HPS的病理驱动

本研究基因芯片分析发现,BDL3W组大鼠肺组织中FABP4基因表达显著上调(FC≥1.5,P≤0.05),GO富集分析进一步显示脂代谢相关基因显著富集,提示脂代谢紊乱可能是HPS早期的重要病理事件,而FABP4是连接脂代谢异常与肺损伤的关键枢纽分子。已有研究表明,肝硬化患者血清中FABP4水平明显升高,并与多种并发症的发生及不良预后密切相关[13]。在本研究中,通过油红O染色观察发现,BDL5W组肝细胞内脂滴数量显著增加,体积增大,且主要聚集在中央静脉周围区域;而在BMS309403干预后,脂滴的数量和体积均明显减少,伴有肝脏病理损伤减轻、血清肝酶指标(AST、ALT)显著下降。上述结果提示,FABP4的高表达与肝脏脂质堆积密切相关。抑制FABP4可有效缓解脂代谢紊乱、减轻脂毒性对肝细胞的损害,从而从源头上削弱HPS的病理驱动机制。这一结论与BDLB组中血清ALT和AST水平显著下降(同BDL5W组相比)的生化数据相互支持。

3.2 在HPS大鼠模型中BMS309403通过打破FABP4-NF-κB正反馈环路解除对PPAR-γ的抑制,从而改善脂代谢与炎症

本研究的核心发现之一是BMS309403干预后,HPS大鼠肺组织FABP4表达显著降低的同时,PPAR-γ表达水平显著上调。这一结果表明,在HPS病理背景下,FABP4对PPAR-γ发挥负向调控作用,抑制FABP4可解除对PPAR-γ的抑制效应。BMS309403的主要作用是抑制FABP4的活性,然而在本研究中出现FABP4表达降低的情况。其可能的机制包括:①改善炎症微环境,减少FABP4高表达细胞浸润。FABP4主要由巨噬细胞和内皮细胞表达[6],且可促进巨噬细胞募集和M1极化[18]。BMS309403减轻肺部炎症后,高表达FABP4的巨噬细胞浸润减少,组织整体FABP4总量随之降低。②打断FABP4-NF-κB p65正反馈环路。FABP4激活NF-κB p65,而NF-κB p65又可上调FABP4转录,形成自我强化循环[18-19]。BMS309403抑制FABP4活性后削弱了对NF-κB p65的激活,该正反馈环路被打破,FABP4转录合成减少。

FABP4与PPAR-γ之间的调控关系并非单一的线性模式。一方面,PPAR-γ是一种依赖配体激活的核受体,属于核激素受体超家族中的转录因子,其在FABP4的转录调控中起关键作用。在脂肪细胞分化过程中,PPAR-γ激活可促进FABP4的表达,从而帮助新生成的脂肪细胞更高效地摄取和储存脂肪酸,减少脂肪在非脂肪组织中的异常沉积所带来的毒性作用[20]。在HBV感染或MASLD相关的肝细胞癌中,PPAR-γ也可驱动FABP4在肿瘤血管内皮细胞中的高表达,通过激活Notch1信号通路促进血管正常化[21]。另一方面,FABP4对PPAR-γ的反向调节作用在不同的病理背景下表现出差异。例如,在人乳腺癌MCF-7细胞中,FABP4能够介导特定配体从细胞质转运至细胞核,促进其与PPAR-γ结合,从而增强PPAR-γ的转录活性[22]。然而,也有研究指出,FABP4可通过诱导PPAR-γ的泛素化并促进其通过蛋白酶体降解,从而抑制其功能并减少脂肪生成[23]。在软骨细胞中,FABP4的表达下调反而能够激活PPAR-γ,抑制NF-κB信号通路,缓解炎症和氧化应激反应[24]。这种双向调控机制可能受到细胞类型、疾病发展阶段及局部微环境等多种因素的影响。在本研究构建的HPS模型中,抑制FABP4表达可显著提升PPAR-γ的表达水平与活性,从而改善脂代谢紊乱和炎症反应,其调控模式与软骨细胞中的观察一致。这提示在以炎症为主导的病理环境下,FABP4更可能对PPAR-γ产生抑制效应。

3.3 在HPS大鼠模型中调控FABP4/PPAR-γ信号轴通过抑制NF-κB/TNF-α通路来减轻iNOS介导的肺微血管扩张与低氧血症

肺内血管扩张和血管新生是HPS的关键病理环节,炎症反应在此过程中发挥核心驱动作用。在全身炎症状态下,NF-κB p65、TNF-α、IL-1β和IL-6等炎症介质的释放不仅导致内皮功能障碍和血管张力调节失衡,还能直接促进肺血管的病理性重塑。本研究发现BDL5W组肺组织NF-κB p65和TNF-α表达显著上调,iNOS表达增加,CD31标记的肺微血管管腔直径明显增大,同时PaO_2下降、$P(A-a)O_2$升高,证实“炎症激活-iNOS/NO生成增加-肺微血管扩张-低氧血症”这一经典HPS病理链条的存在。

在机制层面,FABP4与PPAR-γ分别从促炎和抗炎2个方向调控NF-κB通路,共同决定炎症反应的强度。FABP4可通过增强巨噬细胞活性和促进NF-κB通路活化加剧炎症级联反应[25-26]。NF-κB p65激活后,不仅启动TNF-α、IL-1β和IL-6等促炎基因的转录[27],还可直接诱导iNOS的表达[28]。iNOS产生的高水平NO具有双重病理效应:作为强效血管扩张剂导

致HPS特征性的肺血管过度扩张,引起通气/血流比例失调和低氧血症[4];同时与ROS反应生成过氧亚硝酸盐($ONOO^-$),造成氧化应激和组织损伤[29]。此外,炎症刺激下VEGF等促血管生成因子表达上调[30],促进肺内微血管增殖和重塑,形成通透性高的异常新生血管,进一步加剧肺内分流[31]。

与FABP4的促炎作用相反,PPAR-γ可通过与NF-κB亚基(p50和p65)直接相互作用或招募共抑制因子,抑制NF-κB p65及其依赖性基因的转录,发挥抗炎与血管保护作用[32]。因此,在HPS病理状态下,FABP4表达升高与PPAR-γ活性抑制的叠加效应,削弱了机体对NF-κB p65/TNF-α炎症风暴的内源性抵抗能力,从而加剧肝肺损伤和肺血管扩张。本研究中BMS309403干预后NF-κB p65和TNF-α表达显著下调($P<0.01$),iNOS表达降低,肺微血管管腔直径减小($P<0.01$),PaO_2回升,P(A-a)O_2下降,充分证实了通过调控FABP4/PPAR-γ信号轴抑制NF-κB p65/TNF-α通路可有效缓解HPS的肺部炎症和微血管扩张。

本研究存在一定局限性:①BDL模型主要模拟胆汁淤积性肝硬化,其病理特征与酒精性、病毒性等其他类型肝硬化可能存在差异,研究结论的外推需要谨慎;②本研究主要关注FABP4/PPAR-γ通路,HPS发病涉及的其他信号通路如ET-1/NO平衡、VEGF信号等与FABP4/PPAR-γ轴之间的交互作用尚需进一步探讨;③BMS309403降低FABP4蛋白水平的具体分子机制仍需通过mRNA水平检测和蛋白半衰期实验等方法加以验证。

综上所述,本研究初步证实了FABP4/PPAR-γ信号轴在HPS发病机制中的重要作用。通过抑制FABP4可增强PPAR-γ活化,改善脂代谢紊乱,削弱肺部炎症级联反应,从而减轻HPS大鼠的肝肺损伤,改善肺微血管扩张和低氧血症,为临床开发新的HPS靶向治疗策略提供了重要实验依据。

利益冲突 本文所有作者声明不存在利益冲突

参考文献:

[1] RODRÍGUEZ-ROISIN R, KROWKA M J. Hepatopulmonary syndrome: a liver-induced lung vascular disorder[J]. N Engl J Med, 2008, 358(22): 2378-2387. DOI: 10.1056/NEJMra0707185.

[2] GANDHI K D, TAWEESEDT P T, SHARMA M, *et al*. Hepatopulmonary syndrome: an update[J]. World J Hepatol, 2021, 13(11): 1699-1706. DOI:10.4254/wjh.v13.i11.1699.

[3] ZAKA A Z, MANGOURA S A, AHMED M A. New updates on hepatopulmonary syndrome: a comprehensive review[J]. Respir Med, 2025, 236: 107911. DOI: 10.1016/j.rmed.2024.107911.

[4] RAEVENS S, BORET M, FALLON M B. Hepatopulmonary syndrome[J]. JHEP Rep, 2022, 4(9): 100527. DOI: 10.1016/j.jhepr.2022.100527.

[5] KROWKA M J, FALLON M B, KAWUT S M, *et al*. International liver transplant society practice guidelines: diagnosis and management of hepatopulmonary syndrome and portopulmonary hypertension[J]. Transplantation, 2016, 100(7): 1440-1452. DOI:10.1097/TP.0000000000001229.

[6] SHI Y, WANG C C, WU L Q, *et al*. Pathophysiological insight into fatty acid-binding protein-4: multifaced roles in reproduction, pregnancy, and offspring health[J]. Int J Mol Sci, 2023, 24(16): 12655. DOI:10.3390/ijms241612655.

[7] WU L, OU G L, ZHANG W, *et al*. Fatty acid-binding proteins in cancers[J]. Int J Surg, 2025, 111(11): 8402-8422. DOI:10.1097/JS9.0000000000003049.

[8] CHIYONOBU N, SHIMADA S, AKIYAMA Y, *et al*. Fatty acid binding protein 4 (FABP4) overexpression in intratumoral hepatic stellate cells within hepatocellular carcinoma with metabolic risk factors[J]. Am J Pathol, 2018, 188(5): 1213-1224. DOI: 10.1016/j.ajpath.2018.01.012.

[9] PHAM D V, PARK P H. Tumor metabolic reprogramming by adipokines as a critical driver of obesity-associated cancer progression[J]. Int J Mol Sci, 2021, 22(3): 1444. DOI: 10.3390/ijms22031444.

[10] CHRISTODOULATOS G S, SPYROU N, KADILLARI J, *et al*. The role of adipokines in breast cancer: current evidence and perspectives[J]. Curr Obes Rep, 2019, 8(4): 413-433. DOI:10.1007/s13679-019-00364-y.

[11] GUAITA-ESTERUELAS S, GUMÀ J, MASANA L, *et al*. The peritumoural adipose tissue microenvironment and cancer. The roles of fatty acid binding protein 4 and fatty acid binding protein 5[J]. Mol Cell Endocrinol, 2018, 462(Pt B): 107-118. DOI:10.1016/j.mce.2017.02.002.

[12] HARJES U, BRIDGES E, GHARPURE K M, *et al*. Antiangiogenic and tumour inhibitory effects of downregulating tumour endothelial FABP4[J]. Oncogene, 2017, 36(7): 912-921. DOI:10.1038/onc.2016.256.

[13] GRAUPERA I, COLL M, POSE E, *et al*. Adipocyte fatty-acid binding protein is overexpressed in cirrhosis and correlates with clinical outcomes[J]. Sci Rep, 2017, 7(1): 1829. DOI:10.1038/s41598-017-01709-0.

[14] BOSQUET A, GIRONA J, GUAITA-ESTERUELAS S, *et al*. FABP4 inhibitor BMS309403 decreases saturated-fatty-acid-induced endoplasmic reticulum stress-associated inflammation in skeletal muscle by reducing p38 MAPK activation[J]. Biochim Biophys Acta Mol Cell Biol Lipids, 2018, 1863(6): 604-613. DOI: 10.1016/j.bbalip.2018.

03.004.

[15] CHEN Y T, DAI Y, SONG K X, *et al*. Pre-emptive pharmacological inhibition of fatty acid-binding protein 4 attenuates kidney fibrosis by reprogramming tubular lipid metabolism[J]. Cell Death Dis, 2021, 12(6): 572. DOI: 10.1038/s41419-021-03850-1.

[16] LAOUIREM S, SANNIER A, NORKOWSKI E, *et al*. Endothelial fatty liver binding protein 4: a new targetable mediator in hepatocellular carcinoma related to metabolic syndrome[J]. Oncogene, 2019, 38(16): 3033-3046. DOI: 10.1038/s41388-018-0597-1.

[17] MUKHERJEE A, CHIANG C Y, DAIFOTIS H A, *et al*. Adipocyte-induced FABP4 expression in ovarian cancer cells promotes metastasis and mediates carboplatin resistance[J]. Cancer Res, 2020, 80(8): 1748-1761. DOI: 10.1158/0008-5472.CAN-19-1999.

[18] ZHOU C, SHEN Z Y, SHEN B, *et al*. FABP4 in LSECs promotes CXCL10-mediated macrophage recruitment and M1 polarization during NAFLD progression[J]. Biochim Biophys Acta BBA Mol Basis Dis, 2023, 1869(7): 166810. DOI:10.1016/j.bbadis.2023.166810.

[19] ZHOU X D, ZHOU S H, TAO J, *et al*. HIV-1 Tat drives the Fabp4/NF-κB feedback loop in microglia to mediate inflammatory response and neuronal apoptosis[J]. J Neurovirol, 2022, 28(4/5/6): 483-496. DOI: 10.1007/s13365-022-01094-z.

[20] DOU H X, WANG T, SU H X, *et al*. Exogenous FABP4 interferes with differentiation, promotes lipolysis and inflammation in adipocytes[J]. Endocrine, 2020, 67(3): 587-596. DOI:10.1007/s12020-019-02157-8.

[21] ZHANG S Y, XU H H, LI M W, *et al*. An etiology-stratified single-cell atlas identifies FABP4 as a prognostic marker for MASLD-related HCC[J]. J Hepatol, 2025: S0168-S8278(25)02609-1. DOI: 10.1016/j. jhep. 2025. 10.026.

[22] AYERS S D, NEDROW K L, GILLILAN R E, *et al*. Continuous nucleocytoplasmic shuttling underlies transcriptional activation of PPARgamma by FABP4[J]. Biochemistry, 2007, 46(23): 6744-6752. DOI: 10.1021/bi700047a.

[23] GARIN-SHKOLNIK T, RUDICH A, HOTAMISLIGIL G S, *et al*. FABP4 attenuates PPARγ and adipogenesis and is inversely correlated with PPARγ in adipose tissues[J]. Diabetes, 2014, 63(3): 900-911. DOI:10.2337/db13-0436.

[24] MAO H J, HAN B, LI H, *et al*. FABP4 knockdown suppresses inflammation, apoptosis and extracellular matrix degradation in IL-1β-induced chondrocytes by activating PPARγ to regulate the NF-κB signaling pathway[J]. Mol Med Rep, 2021, 24(6): 855. DOI: 10.3892/mmr.2021.12495.

[25] XU L B, ZHANG H P, WANG Y H, *et al*. FABP4 activates the JAK2/STAT2 pathway *via* Rap1a in the homocysteine-induced macrophage inflammatory response in ApoE(-/-) mice atherosclerosis[J]. Lab Invest, 2022, 102(1): 25-37. DOI:10.1038/s41374-021-00679-2.

[26] ODDI S, SCIPIONI L, TOTARO A, *et al*. The anti-inflammatory agent bindarit acts as a modulator of fatty acid-binding protein 4 in human monocytic cells[J]. Sci Rep, 2019, 9(1): 15155. DOI:10.1038/s41598-019-51691-y.

[27] FACCHIN B M, DOS REIS G O, VIEIRA G N, *et al*. Inflammatory biomarkers on an LPS-induced RAW 264.7 cell model: a systematic review and meta-analysis[J]. Inflamm Res, 2022, 71(7/8): 741-758. DOI: 10.1007/s00011-022-01584-0.

[28] CHEN H Q, HU Q Y, WEN T, *et al*. Arteannuin B, a sesquiterpene lactone from *Artemisia annua*, attenuates inflammatory response by inhibiting the ubiquitin-conjugating enzyme UBE2D3-mediated NF-κB activation[J]. Phytomedicine, 2024, 124: 155263. DOI: 10.1016/j.phymed.2023.155263.

[29] JOMOVA K, ALOMAR S Y, ALWASEL S H, *et al*. Several lines of antioxidant defense against oxidative stress: antioxidant enzymes, nanomaterials with multiple enzyme-mimicking activities, and low-molecular-weight antioxidants[J]. Arch Toxicol, 2024, 98(5): 1323-1367. DOI: 10.1007/s00204-024-03696-4.

[30] SOULAIDOPOULOS S, CHOLONGITAS E, GIANNAKOULAS G, *et al*. Review article: update on current and emergent data on hepatopulmonary syndrome[J]. World J Gastroenterol, 2018, 24(12): 1285-1298. DOI:10.3748/wjg.v24.i12.1285.

[31] CHEN L, HAN Y, LI Y J, *et al*. Hepatocyte-derived exosomal miR-194 activates PMVECs and promotes angiogenesis in hepatopulmonary syndrome[J]. Cell Death Dis, 2019, 10(11): 853. DOI: 10.1038/s41419-019-2087-y.

[32] CARVALHO M V, GONÇALVES-DE-ALBUQUERQUE C F, SILVA A R. PPAR gamma: from definition to molecular targets and therapy of lung diseases[J]. Int J Mol Sci, 2021, 22(2): 805. DOI:10.3390/ijms22020805.

(收稿:2026-01-30;修回:2026-03-30)

(编辑 汤锦波)